A mapping of martian water sublimation during early northern summer using OMEGA/Mars Express

T. Encrenaz[1], R. Melchiorri[1], T. Fouchet[1], P. Drossart[1], E. Lellouch[1], B. Gondet[2], J.-P. Bibring[2], Y. Langevin[2], D. Titov[3], N. Ignatiev[4], and F. Forget[5]

1. LESIA, Observatoire de Paris, 92195 Meudon, France
   e-mail: Therese.Encrenaz@obspm.fr
2. Institut d'Astrophysique Spatiale, Orsay Campus, 91405 Orsay, France
3. MPI, Max-Planck St. 2, 37191 Katlenburg-Lindau, Germany
4. IKI, Profnoyuznaya 87/32, Moscow 117997, Russia
5. IPSL/LMD, place Jussieu, 75231 Paris cedex 05, France

Received 13 July 2005 / Accepted 9 August 2005

ABSTRACT

The OMEGA imaging spectrometer aboard Mars Express has been used to map the water vapor abundance over the martian surface, from the analysis of the 2.6 μm band of H_2O. As a preliminary result of this study, we present water vapor maps in the northern hemisphere at the time of the northern polar cap sublimation ($Ls = 94$–112 deg). The maps show a mean H_2O mixing ratio of about 2–3×10^{-4} at a latitude of 40N, and in the range of 5×10^{-4}–10^{-3} at 60N–80N latitudes. The corresponding mean H_2O column densities are about 25 pr-μm at 40N and between 40 and 60 pr-μm at 60N–80N, with uncertainties of about 30 percent. Our results are in agreement with previous results by MAWD/Viking and TES/MGS for latitudes up to 60N, but seem to indicate lower values at high latitude. However they are still globally consistent in view of our error bars.

Key words. planets and satellites: Mars – infrared: solar system

1. Introduction

Water vapor on Mars is known to exhibit a complex seasonal cycle, associated to the periodic condensation and sublimation of H_2O on each polar cap. Seasonal variations of water vapor on Mars have been monitored by the IRIS instrument aboard Mariner 9 (Conrath et al. 1973), then by the MAWD (Mars Atmospheric Water Detection) experiment (Farmer et al. 1977; Jakosky & Farmer 1982; Fedorova et al. 2004) aboard the Viking orbiters. These observations have shown evidence for large spatial and temporal variations of the water column density, with maxima as high as 80 pr-μm, at high northern latitudes, at the time of early northern summer ($Ls = 100$–120 deg) and minima as low as 1–3 pr-μm in the opposite hemisphere at the same time (Jakosky & Haberle 1992).

The MAWD experiment aboard Viking used a weak H_2O absorption band near 1.38 μm, while the IRIS analysis was based upon rotational H_2O transitions beyond 20 μm. Since the Viking observations, maps of the water vapor on Mars have been obtained by the Thermal Emission Spectrometer (TES) aboard the MGS (Mars Global Surveyor) spacecraft (Smith 2002, 2004). In the TES study, as in the case of the IRIS analysis from Mariner 9, the water content was retrieved from the

study of thermal H_2O rotational lines. This method requires the knowledge of the temperature profile, retrieved from the inversion of the CO_2 ν_2 band at 15 μm. The OMEGA instrument aboard the Mars Express orbiter offers an alternative method for retrieving the water vapor abundance through the analysis of the (ν_1, ν_3) bands of H_2O at 2.6 μm. As these bands appear in the reflected sunlight component of the spectrum, this analysis, like the method used by MAWD, has the advantage of being, to first order, independent of the temperature profile. It also applies to the polar caps where thermal measurements are not possible. In this letter, we present a study of the water vapor abundance of Mars at the time of its maximum abundance in the seasonal cycle, when the H_2O seasonal northern cap starts to sublimate during early northern summer ($Ls = 94$–112 deg).

2. The OMEGA instrument aboard Mars Express

The Mars Express spacecraft, launched by ESA on June 2, 2003, has been operating in a quasi-polar orbit around Mars since January 2004. Aboard Mars Express, the OMEGA imaging spectrometer operates from the visible (0.3 μm) to the thermal infrared (5.2 μm) with a spectral sampling of 7 nm below 1 μm, 14 nm in the 1.0–2.5 μm range, and 20 nm above 2.5 μm. Its instantaneous field of view (IFOV) of 1.2 mrad

corresponds to about 300 m at the martian surface near periapsis. The crosstrack FOV (perpendicular to the spacecraft motion) varies from 16 to 128 IFOV depending on the operating mode of the observing sequence.

Figure 1 shows the ratio of two averaged OMEGA spectra between 1.0 and 2.7 μm, recorded at the foot and at the summit of Olympus Mons respectively (Orbit 37-3). This ratio exhibits strong absorption features, mostly due to CO$_2$. Indeed, the CO$_2$ absorption bands are stronger on the Olympus foot spectrum because the CO$_2$ column density above the surface is larger. In order to eliminate the uncertainty associated with the OMEGA instrumental transfer function, we have divided each individual spectrum by the averaged spectrum of the Olympus summit, taken as a reference. This method can be applied because of the great stability of the instrumental parameters over the whole observing period.

3. Modelling of the atmospheric spectrum

The absorption due to the martian atmospheric gases was calculated over the 1.0–2.7 μm range, using a line-by-line radiative transfer code including the spectral signatures of CO$_2$, H$_2$O and CO. Spectroscopic parameters were taken from the GEISA data bank (Jacquinet-Husson 1999). Line-broadening parameters for CO$_2$–CO$_2$ collisions and H$_2$O–CO$_2$ collisions were taken from (Pollack et al. 1993) and references therein. The atmospheric parameters were taken from the Global Climate Model (GCM) developed at LMD-Oxford (Forget et al. 1999). For the calculations corresponding to the Olympus Mons spectra (Orbit 37-3; Ls = 337 deg), the surface temperature was in the range 275–280 K; the assumed atmospheric temperature was 250 K at P = 7.5 mbars, 200 K at 1.6 mbars, and about 150 K at pressures lower than 0.1 mbar (at altitudes higher than 45 km). Calculations were performed with a frequency step of 0.01 cm^{-1}, then convolved with the OMEGA instrumental function.

In Fig. 1, the ratio of the Olympus foot spectrum by the Olympus summit spectrum is compared to a set of synthetic models. The CO$_2$ signatures are strong at 2.75 ($\nu_1 + \nu_3$) and 2.0 μm ($2\nu_1 + \nu_3$), while weaker bands appear at 1.44 μm ($3\nu_3$) and 1.6 μm ($3\nu_1 + \nu_3$). H$_2$O shows a clear signature at 2.6 μm (ν_1, ν_3, in the wing of the strong CO$_2$ band at 2.7 μm) while two weaker water features appear at 1.38 μm ($\nu_1 + \nu_3$) and 1.9 μm (hydratation band). The 2.6 μm band is most favorable because it is a factor 3 to 5 times stronger than the other ones, and because the 2.6 μm spectral range is expected to be free of mineralogic signatures.

4. Analysis of the 2.6 μm H$_2$O band

In order to determine the atmospheric parameters associated to the reference spectrum, we have used the MOLA data to determine the altitude of the spectra locations, at the summit and at the foot of Olympus Mons respectively, and the GCM thermal profile associated to this region. Following the GCM database, we used a surface pressure of 1.1 mbar at the Olympus summit and, from the best fit of the CO$_2$ bands (Fig. 1), we inferred a surface pressure of 7.5 mbar at the location of the
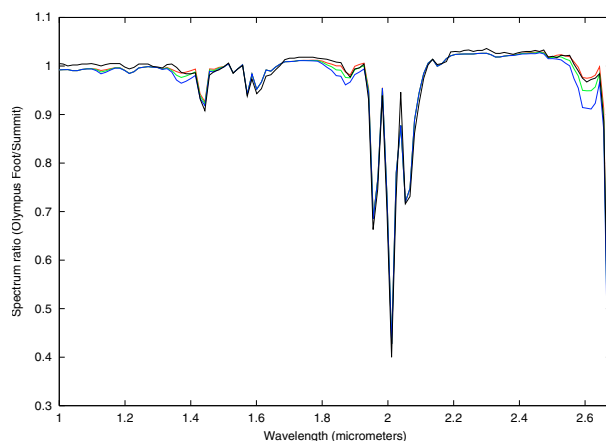

Fig. 1. Black curve: ratio of two averaged OMEGA raw spectra, recorded at the foot (lat = 30N, long = 227E) and at the summit (lat = 17N, long = 227E) of Olympus Mons respectively (Orbit 37-3). Each spectrum is the average of 352 individual spectra, corresponding to 11 pixels along the latitude (spacecraft motion) and 32 pixels along the longitude. Color curves: synthetic ratio of spectra calculated with averaged Ps values of 1.1 mbar at the summit and 7.5 mbar at the foot. A constant mixing ratio is assumed for Q(H$_2$O). Red: Q(H$_2$O = 150 ppm; green: Q(H$_2$O) = 300 ppm; blue: Q(H$_2$O) = 600 ppm. The best fit is achieved for Q(H$_2$O) = 150 ppm.

foot spectrum; this value is also in good agreement with the GCM predictions. We then assumed a constant mixing ratio of H$_2$O at the two locations, and we inferred an H$_2$O mixing ratio of 150 ppm from the best fit of the 2.6 μm H$_2$O band. This allows us to calculate a synthetic spectrum associated to our reference spectrum. The corresponding H$_2$O column density is 1.6 pr-μm.

It has to be mentioned that there is some uncertainty associated with the assumption of a constant mixing ratio over the Olympus region. If the H$_2$O mixing ratio at the summit were twice its value at the foot, the corresponding column density at the summit would be 3.2 pr-μm, while it could be as low as zero if H$_2$O were significantly depleted at the summit. However, as the expected abundances of H$_2$O are above 50 pr-μm at high northern latitude at the time of the northern polar cap sublimation, this uncertainty should be less than a few percent.

Synthetic calculations show that the depths of the H$_2$O bands depend not only upon the H$_2$O column density but also upon the pressure. In order to infer the water vapor content from the OMEGA data, one must also determine the surface pressure corresponding to each individual spectrum. A possible method could be to study the variations of the depth of the weak CO$_2$ band at 1.44 μm as a function of the surface pressure. However, this method has two inconvenients. First, for large water contents, the 1.44 μm CO$_2$ band is contaminated by the 1.38 μm H$_2$O band (Fig. 1). Second, the CO$_2$ gaseous bands cannot be used if water ice is present (Fig. 2) due to the presence of strong and broad absorption bands centered at 1.5 μm and 2.0 μm. Water ice extends at northern latitudes higher than 80N (Langevin et al. 2005). For these reasons, we have used the surface pressure predicted by the GCM on the basis of the MOLA data.
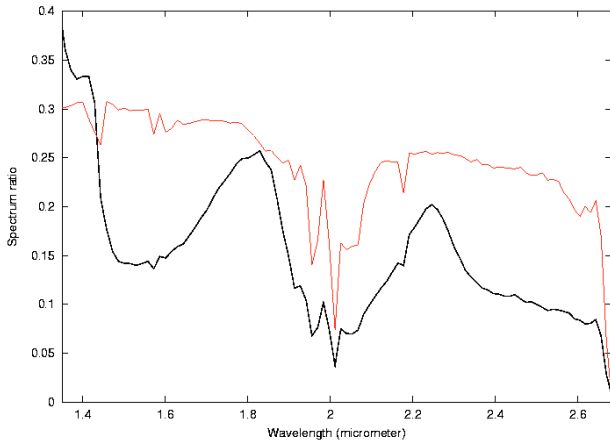
Fig. 2. Black line: a spectrum of Mars (divided by the reference spectrum of Olympus summit) recorded on Orbit 902-1 (lat. above 80N) showing two strong and broad bands at 1.5 μm and 2 μm, characteristic of water ice. Red line: another spectrum of the same orbit (divided by the same reference), taken at a lower northern latitude (below 80N), is also shown for comparison; the water ice bands are absent.

In order to infer the water content from the depth of the 2.6 μm H₂O band, we have built a grid of curves of growth using as entry parameters the H₂O mixing ratio Q at the surface and the surface pressure Ps. The temperature profile was inferred from the GCM corresponding to the conditions of Orbit 37-3, which was used for validating our calculations.

Our method has then been applied to the conditions of early northern summer by using the relevant atmospheric temperature profile. This profile was selected from the GCM as a mean value of $T(z)$ at high northern latitudes (65 N), averaged over longitude, for Ls = 90–120 deg. This thermal profile is significantly colder than the first one we used (corresponding to the conditions of Orbit 37, Ls = 337 deg), with a maximum difference of about 10 K (for a given pressure) in the lower atmosphere (below 10 km). The new surface temperature Ts (240 K) is about 40 K lower than its value on Olympus Mons at the time of the OMEGA observations. Nevertheless, calculations show that the temperature has a very minor effect on the H₂O depth at 2.6 μm, as the calculated depth varies at maximum by 2–3 percent over the whole range of atmospheric parameters. As a result, the difference in the H₂O column density is 3 pr-μm for an H₂O content of 80 pr-μm. As mentioned above, we used for eachs spectrum the surface pressure interpolated from the GCM grid.

5. Results

Figures 3–5 show 3 maps of the H₂O mixing ratio in the northern region for different values of Ls. Mean values are in the range of 2–3 × 10⁻⁴ at a latitude of 40N, and 5–10 × 10⁻⁴ at 60N–80N.

The measurement of the water vapor mixing ratio at the surface allows to infer directly the sublimation rate of H₂O (if the surface temperature is known), independently of the altitude of the observed location. It is also interesting to convert our results in terms of water vapor column density (which is actually the
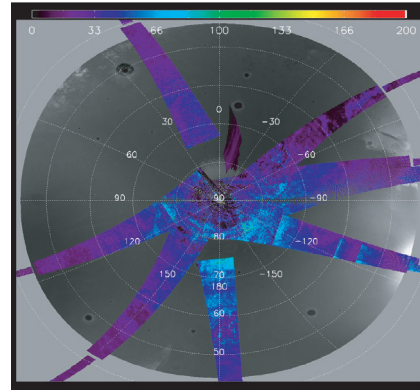

Fig. 3. The H₂O mixing ratio at high northern latitudes for Ls = 94 deg. The projection is centered on the north pole. Northern latitudes are indicated at the center of the figure, and eastern longitudes are shown along the 70N parallel. The scale of the H₂O mixing ratio ranges from 0 to 2 × 10⁻³. A mixing ratio of 10⁻³ corresponds to a column density of about 65 prμm. This figure includes data from orbits 886–888, 891, 892, 894, 895, 898, 902, 905, 907, 909.
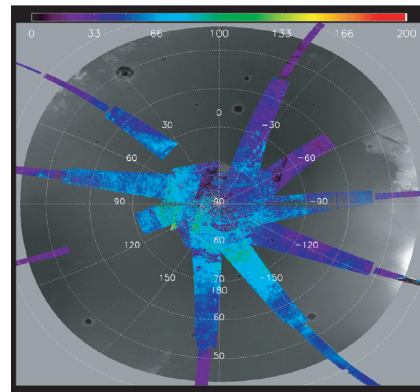

Fig. 4. Same as Fig. 3, with Ls = 102.5 deg. This figure includes data from orbits 946, 954, 955, 961, 962, 964–967, 970–972 .
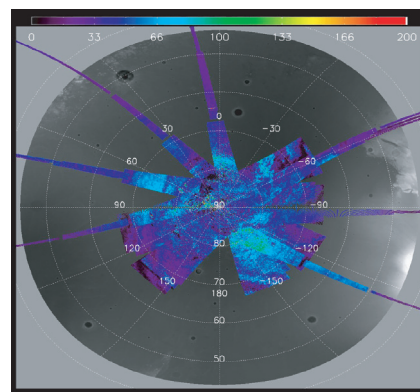

Fig. 5. Same as Fig. 3, for Ls = 112 deg. This figure includes data from orbits 1026, 1029, 1030, 1032, 1034, 1037, 1040, 1041, 1043, 1047, 1048, 1050.

observed parameter), for comparison with other measurements using this unit. For this we need to know the surface pressure of each spectrum. As shown by the GCM data, the surface pressure at 70N–80N typically ranges between 7.5 and 9.5 mbars. Figure 6 shows the relationship between the H₂O surface
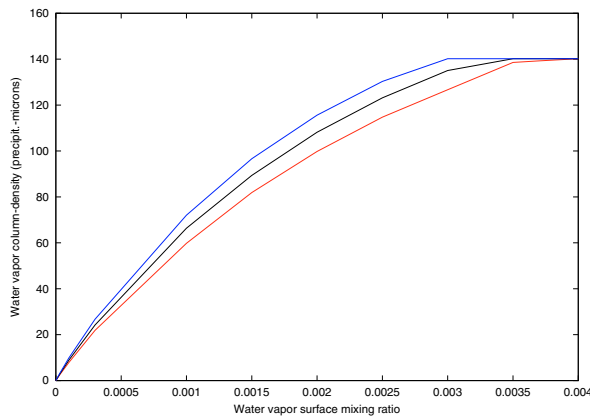
Letter to the Editor

Fig. 6. The water vapor column density as a function of its surface mixing ratio. Surface pressures: 7.5 mbars (red), 8.5 mbars (black), 9.5 mbars (blue).

mixing ratio and the H_2O column density in pr-μm, assuming $Ts = 240$ K, $T(z = 0) = 220$ K, and 3 values of Ps (7.5, 8.5 and 9.5 mbars). Saturation becomes to play a role for column densities higher than about 20 pr-μm. As the water content increases, saturation occurs at lower and lower altitudes, to reach the zero altitude level for surface mixing ratios higher than 3.5×10^{-3}. The corresponding column density would be 140 pr-μm. For a surface pressure of 7.5 mbars, a water mixing ratio of 1.5×10^{-3} (corresponding to 80 pr-μm) corresponds to a saturation altitude of about 6 km.

6. Discussion

Our results on the water vapor abundance can be compared to those of Viking Jakosky & Haberle (1992) and TES (Smith 2002, 2004). From Figs. 3–5, we infer, at 40N latitude range, a mean H_2O column density of 20–25 pr-μm, approximately constant over the 94–112 deg Ls range. The corresponding values are also between 20 and 25 pr-μm for both TES Smith (2004) and Viking. At 60N, we derive an H_2O content between about 25 pr-μm ($Ls = 94$ deg) and 45 pr-μm ($Ls = 112$ deg), to be compared with Viking and TES (Smith 2004) values increasing from 30 to 50 pr-μm. At 80N, our results appear to be lower than TES and Viking with a mean maximum column density of about 55 pr-μm, while maximum values of 75 and 80 pr-μm were reported by Smith (2002) and Jakosky & Haberle (1992). The GCM measurements are in general agreement with the TES results.

The uncertainty on our results has several sources (signal/noise ratio, temperature profile, modelling, surface pressure, water content over Olympus Mons, incomplete longitude coverage). The uncertainty on the H_2O line depth, in an individual spectrum, ranges between 10 and 25 percent, depending upon the continuum level (see Fig. 2), and is probably our major source of error. We take a conservative estimate of about 30 percent our global uncertainty. In view of this error bar, there is no strong evidence for interannual variations of the maximum water vapor column density, although our results for $Ls = 112$ deg could indicate a lower H_2O content as compared to the previous years. A more refined analysis of the OMEGA data will be needed to confirm this tendency.

In summary, the retrieval of the water vapor column density from the 2.6 μm reflected band of H_2O appears to be a powerful and promising method for measuring the water vapor content of Mars. This preliminary study will be completed in the future using a larger dataset, and will be later extended to monitor the water vapor abundance over the whole seasonal cycle at all latitude ranges.

References

Conrath, B. J., Curran, R., Hanel, R., et al. 1973, J. Geophys. Res., 78, 4267

Farmer, C. B., Davis, D. W., Holland, A. L., et al. 1977, J. Geophys. Res., 82, 4225

Fedorova, A. A., Rodin, A. V., & Baklanova, I. V. 2004, Icarus, 171, 54

Forget, F., Hourdin, F., Fournier, R., et al. 1999, J. Geophys. Res., 104, 24155

Jacquinet-Husson, N., et al. 1999, J. Quant. Spectr. Rad. Transfer, 62, 205

Jakosky, B. M., & Farmer, C. B. 1982, J. Geophys. Res., 87, 2999

Jakosky, B. M., & Haberle, R. M. 1992, in Mars, ed. H. H. Kieffer et al. (University of Arizona Press)

Langevin, Y., Poulet, F., Bibring, J.-P., et al. 2005, Science, 307, 1581

Pollack, J. B., Dalton, J. B., Grinspoon, D., et al. 1993, Icarus, 103, 1

Smith, M. D. 2002, J. Geophys. Res., 107, E11, 5115, doi:10.1029/2001/JE001522

Smith, M. D. 2004, Icarus, 167, 148